Appl. Phys. B 70, 261–265 (2000) / Digital Object Identifier (DOI) 10.1007/s003409900161

Applied Physics B
Lasers
and Optics

Photoluminescence in anatase titanium dioxide nanocrystals

W.F. Zhang, M.S. Zhang, Z. Yin, Q. Chen

National Laboratory of Solid State Microstructures and Center for Materials Analysis, Nanjing University, Nanjing 210093, P.R. China
(Fax: +86-25/359-5535, E-mail: mszhang@nju.edu.cn)

Received: 7 April 1999/Revised version: 23 August 1999/Published online: 30 November 1999

Abstract. Titanium dioxide (TiO_2) nanocrystals were prepared by a hydrolysis process of tetrabutyl titanate. X-ray diffraction and Raman scattering showed that the as-prepared TiO_2 nanocrystals have anatase structure of TiO_2, and that the monophase anatase nanocrystals can be achieved through a series of annealing treatments below 650 °C. We measured photoluminescence (PL) spectra of the TiO_2 nanocrystals. Under 2.41–2.71 eV laser irradiation, the TiO_2 nanocrystals displayed strong visible light emission with maxima of 2.15–2.29 eV even at excitation power as low as 0.06 W/cm^2. To identify the PL mechanism in the TiO_2 nanocrystals, the dependences of the PL intensity on excitation power and irradiation time were investigated. The experimental results indicated that the radiative recombination is mediated by localized levels related to surface defects residing in TiO_2 nanocrystallites.

PACS: 61.46.+w; 78.30.Hv; 78.55.Hx

Bulk TiO_2 is a wide band-gap semiconductor material of great interest for fundamental research as well as for applications in humidity, oxygen sensitivity, catalysis, and solar energy conversion [1, 2]. The tetragonal rutile modification of TiO_2 has been extensively studied for many years because it is the stable phase at high temperature, and is obtained in most attempts to grow TiO_2 crystals. Contrarily, the tetragonal anatase state of TiO_2 has attracted little attention since people usually hold that anatase should be very similar to rutile in electronic properties. As a result, there are fewer experimental data related to the electronic structure and physical properties of anatase. Nevertheless, the anatase phase can also be stabilized in the form of powders, ceramics, natural or synthetic crystals, and thin films and so on. The increasing interest in anatase is demonstrated by the recent successful application of colloidal anatase in a novel photochemical solar cell and by the discovery of some of its particular properties such as a nonmetal–metal transition in the impurity band of heavily reduced anatase thin films [3, 4]. Photoluminescence (PL) spectroscopy as an important tool has been used to study the electronic structure, optical, photochemical, and photoelectric conversion properties in the rutile and anatase phase of TiO_2 single crystals, thin films, and polycrystalline powders. In rutile crystals, band-gap excitation results in either Wannier-type free exciton emission if the crystal is pure enough, or infrared emission from Cr^{3+} centers [5, 6], whereas in anatase crystals and thin films, band-gap excitation causes the broad-band visible emission which has been interpreted as the radiative recombination of self-trapped excitons localized within TiO_6 octahedra [4, 7]. In TiO_2 polycrystalline powders [8], broad-band visible emission has also been found, and attributed to luminescence from surface states.

Recently, TiO_2 nanocrystals have attracted much attention due to their unique dielectric, optical, and mechanical properties as well as numerous potential applications including photocatalysis, optical coating, and photoelectrochemical solar cells [9–11]. The anatase-to-rutile structural transformation in TiO_2 nanocrystals has been investigated by X-ray diffraction and Raman scattering [12, 13]. The results showed that grain size has a large influence on their structural transformation and basic vibrational properties [14–16]. PL investigations for TiO_2 nanocrystals have also been published by several authors [17, 18], where the revealed luminescence with band-gap excitation was attributed to quantum size effects. This study deals with the preparation of anatase TiO_2 nanocrystals by a hydrolysis process, and the PL properties of TiO_2 nanocrystals excited by visible light with energy lower than the band gap of anatase TiO_2 (3.2 eV) [7]. These results show that anatase TiO_2 nanocrystals possess interesting luminescence characteristics and have potential applications in photocatalysis and photoelectric chemical conversion using visible light.

1 Experimental

TiO_2 nanocrystals were prepared from a chemical solution process: an ethanol solution of tetrabutyl titanate, $Ti(OC_4H_9)_4$, was slowly added into deionized water which was vigorously stirred. The resulting precipitates were repeat-

edly washed with deionized water, followed by evaporation in vacuum at room temperature for a few days. X-ray diffraction (XRD) showed that the as-prepared TiO_2 nanocrystals have pure anatase phase structure. Various grain-size TiO_2 nanocrystals were achieved through a series of annealing treatments in air at temperatures from 100 to 650 °C for 1 h. The average grain size was calculated with the XRD data via the Scherrer's equation, $D = k\lambda/\beta\cos\theta$ [19]. The obtained values are as follows: for the as-prepared nanocrystals the grain size is 6 nm, and for the nanocrystals annealed at 100, 200, 300, 400, 500, 600, and 650 °C, the grain sizes are 7, 9, 12, 16, 22, 27, and 32 nm, respectively.

Raman scattering and PL signals were collected by use of a Spex 1403 Raman spectrometer with a backscattering geometry. An argon-ion laser was used as the excitation light source. In order to facilitate measurements and to ensure the same experimental conditions for the different samples, the nanocrystalline powders were compacted into pellets of 12 mm in diameter and 0.4 mm in thickness under a pressure of 3×10^8 Pa. The density of the pellets is about 2.35 g/cm^3. The sample position was kept unchanged in the measurements.

2 Results and discussion

Figure 1a shows the Raman spectrum for the as-prepared TiO_2 nanocrystals taken with the 488-nm laser line. It is typical of the anatase TiO_2 phase, but with the broader and blueshifted peaks with respect to those of bulk anatase. The broadening and blueshift of the Raman peaks were also found in TiO_2 nanocrystals by other authors, and were attributed to surface pressure or phonon confinement effects that usually exist in nanometer-sized materials [13, 16]. The Raman peaks observed at 151, 409, 515, and 633 cm^{-1} can be assigned as the E_g, B_{1g}, A_{1g} or B_{1g}, and E_g modes of anatase phase, respectively. The occurence of 151 cm^{-1} mode indicates that the as-prepared TiO_2 nanocrystals possess a certain degree of long-range order of the anatase phase, whereas the weak broader peaks in the high-frequency region indicate that they are lack of short-range order. Figure 1b shows the Raman spectrum of the TiO_2 nanocrystals annealed at 650 °C. It is seen that all the Raman peaks are intensified and sharpened after annealing. In addition, a weak peak at 196 cm^{-1}, which belongs to the E_g mode of anatase phase, appears at the high-frequency side of the lowest-frequency E_g mode. These observations manifest the enhancement of short-range order and the evolution of the anatase phase in the TiO_2 nanocrystals towards bulk anatase with annealing. It is also seen that there are a weak peak at 450 cm^{-1} and a small shoulder around 610 cm^{-1} in the Raman spectrum shown in Fig. 1b. They are the E_g and A_{1g} modes of rutile phase, respectively. The appearance of the rutile Raman modes indicates the begining of the anatase-to-rutile transformation at 650 °C annealing. Therefore, annealing temperatures should be controlled below 650 °C to obtain monophase anatase TiO_2 nanocrystals.

The lowest-frequency E_g mode is known to be closely related to the grain size of the TiO_2 nanocrystals. The E_g mode blueshifts in frequency and increases in linewidth with a decrease of grain size [16]. Figure 2 shows the dependence of the E_g mode lineshape (relative intensity, frequency, and linewidth) on annealing treatment. It can be clearly seen from Fig. 2 that as the annealing temperature was increased, the frequency and linewidth of the E_g were redshifted and decreased, respectively, which indicates an increase of grain sizes of TiO_2 nanocrystals upon annealing. These results are in good agreement with the above Scherrer calculations. According to this, the E_g mode of the as-prepared nanocrystals with 6 nm diameter should have the largest linewidth in all of the nanocrystal samples. The obtained linewidth values from Figs. 1 and 2 confirm this conclusion. Hence, the Raman spectra of TiO_2 nanocrystals can be used to estimate qualitatively the increase in grain size upon annealing.

Figure 3 shows the PL spectra for the TiO_2 nanocrystals with different grain sizes. The used excitation photon energy is 2.6 eV (476.5 nm laser line) with a power 0.06 W/cm^2. These spectra have a similar Gaussian-type distribution which

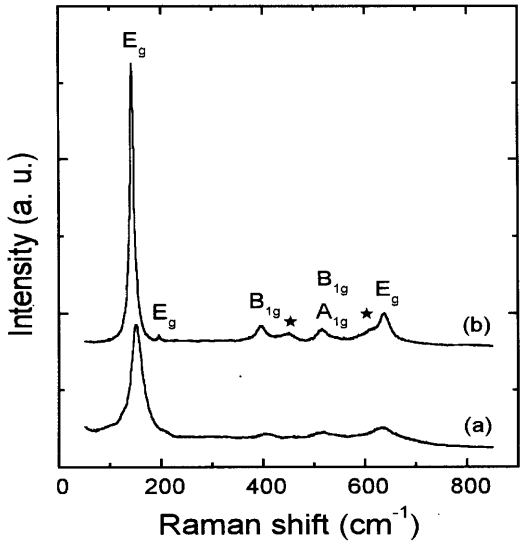

Fig. 1. Raman spectra of TiO_2 nanocrystals: (a) as-prepared and (b) after annealing at 650 °C for 1 h

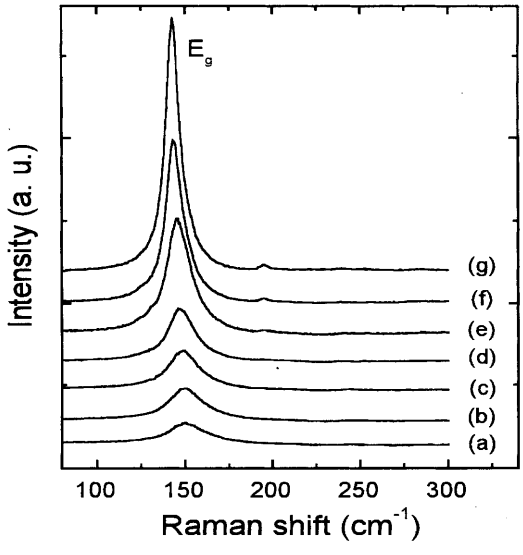

Fig. 2. Lowest-frequency E_g modes for TiO_2 nanocrystals after annealing at (a) 100 °C, (b) 200 °C, (c) 300 °C, (d) 400 °C, (e) 500 °C, (f) 600 °C, and (g) 650 °C for 1 h

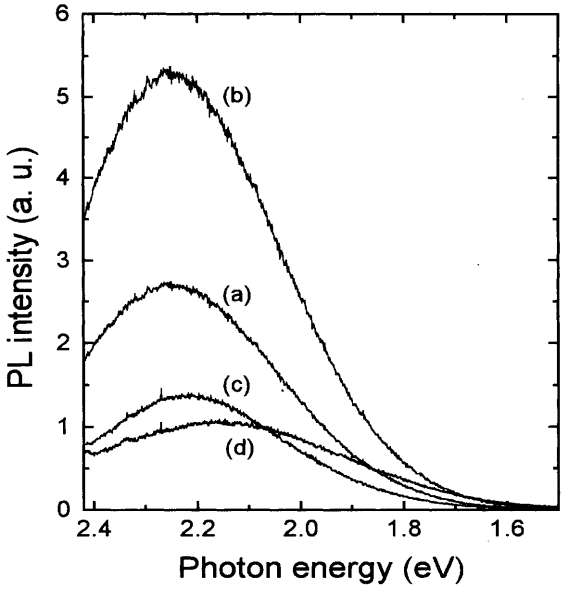

Fig. 3. PL spectra of TiO_2 nanocrystals with different grain sizes: (a) 9 nm, (b) 12 nm, (c) 16 nm, and (d) 27 nm (Excitation: 2.6 eV)

is a broad nonstructure band centered at 2.20±0.04 eV with a halfwidth of 441±40 meV. From Fig. 3, it is clearly seen that the PL peak intensity and position do not change regularly with decreasing grain size. In the case of semiconductor CdS and CuCl nanocrystals, the luminescence spectra showed that as the grain size decreased, the luminescence efficiency was enhanced and the maximum of the emission band was blueshifted [20, 21]. These phenomena related to grain sizes have successfully been explained with a quantum confinement model [22]. However, such a PL dependence on grain size was not found in the anatase TiO_2 nanocrystals. This indicates that the broad visible emission observed here appears not to result from the quantum confinement effect in semiconductor nm-sized systems. Figure 4 shows the PL spectra for the TiO_2 nanocrystals with a grain size of 12 nm under 2.6-eV excitation at several powers. The weak peaks around 2.52 eV appearing in the high-energy side of the curves (c) and (d) belong to the Raman signal (E_g mode, 633 cm^{-1}) of the samples. The PL is obviously intensified for increased excitation power. However, the PL spectral shape does not have evident changes with increasing excitation power. Shown in Fig. 5 is a more distinct dependence of the PL peak intensity (I_{PL}) on excitation power (P) and its approximation by a power-law function $I_{PL} \approx P^{\gamma}$. The dependence has an overall sublinear character. At the lower excitation powers a linear relationship is observed ($\gamma = 1$), whereas at the higher powers it becomes sublinear with $\gamma = 0.5$.

The above results support the assumption that radiative recombination in TiO_2 nanocrystals is mediated by some surface states. The following observations point to this conclusion. First, the energy of radiative recombination is considerably less than the expected energy of optical transitions between the quantum-confined levels for TiO_2 nanocrystals. Second, the sublinear dependence of PL intensity on the excitation power indicates that the recombination is mediated by some localized centers which saturate at high excitation powers [23] and thus let charge carriers recombine via competing nonradiative channels. In the opposite case of excitonic recombination in quantum dots, the saturation of the ground-level PL is accompanied by the onset of the PL of the excited states of the dots [24, 25]. A sublinear dependence should not be expected for the recombination between quantum-confined levels in TiO_2 nanocrystals in our experimental conditions, since we do not observe any change in the spectral shape of the band with excitation power. From Figs. 3 and 4, we also observed that the PL spectra of the TiO_2 nanocrystals resemble those of anatase thin films, crystals, and powders [4, 7, 8]. These spectra all comprise broad and structureless luminescence bands, however, they have different origins. The visible emission caused by band-gap excitation in anatase crystals and thin films has been assigned to the radiative recombination of self-trapped excitons, characteristic of the broad and structureless band, as also observed

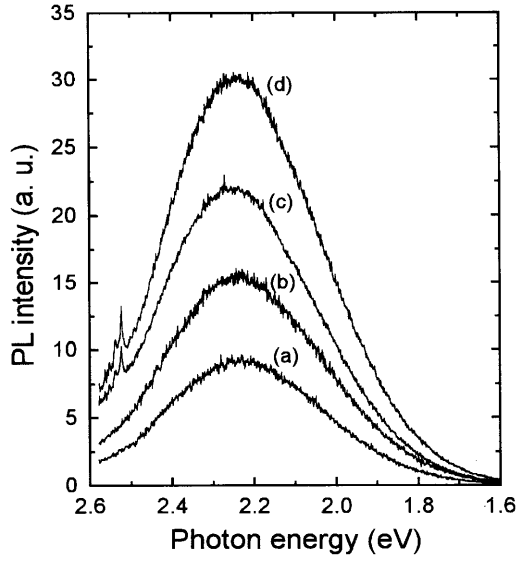

Fig. 4. PL spectra of TiO_2 nanocrystals with a grain size of 12 nm at several excitation powers: (a) 0.11, (b) 0.18, (c) 0.25, and (d) 0.40 W/cm^2 (Excitation: 2.6 eV)

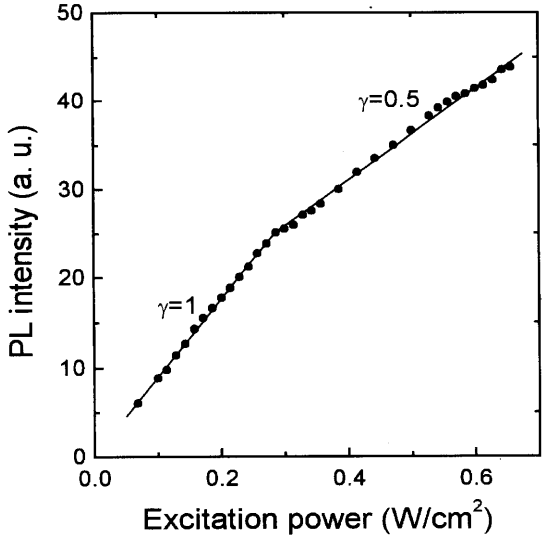

Fig. 5. PL peak intensity as a function of excitation power for TiO_2 nanocrystals with a grain size of 12 nm (Excitation: 2.6 eV)

in several titanates containing TiO_6 octahedra such as $SrTiO_3$ and $BaTiO_3$ crystals [26, 27]. The self-trapped exciton emission is due to strong lattice relaxation and small exciton bandwidth in anatase, and has a large Stokes shift of about 0.9 eV [4, 7]. The visible emission observed in the present work should not be explained as the self-trapped exciton luminescence since it has a small energy difference between the excitation photon energy and the emission maximum. The PL properties in anatase nanocrystals are very similar to those in TiO_2 polycrystalline powders [8]. The surface states should be considered as an important origin responsible for the observed luminescence.

The PL spectra under excitation with the same power at different photon energies were also measured in the TiO_2 nanocrystals with a grain size of 12 nm. Figure 6 shows the dependence of the PL maximum and PL intensity on the excitation photon energy. As the excitation photon energy was increased from 2.41 to 2.71 eV, the PL maximum was blueshifted from 2.15 to 2.29 eV while the PL peak intensity has small variation. This indicates that a series of localized levels within the forbidden gap have a distribution and are suitable for luminescence, and that these levels might have nearly the same luminescence efficiency.

It is worth mentioning that the PL exhibited a large intensity decay with irradiation time. Under laser irradiation, the surface composition and structure of the sample might be damaged due to the effect of overheating and thus lead to the luminescence efficiency decay. However, this mechanism is negligible since the used irradiation power was as low as 0.06 W/cm^2. Therefore, it is suggested that the electronic structures of the surface states of the TiO_2 nanocrystals had a remarkable light-induced change which caused the PL decay with irradiation time. This light-induced change was expected to be reversible. After the TiO_2 sample was kept in the dark for about 2 days, the PL efficiency was well restored. Recently, a similar light-induced change was reported in thin

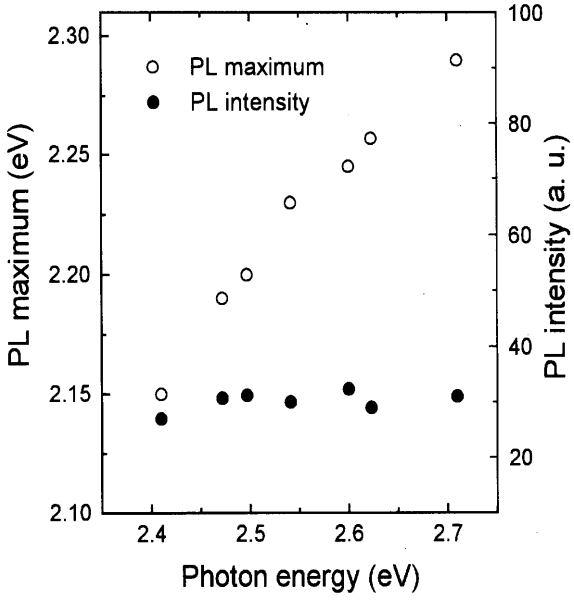

Fig. 6. Dependence of PL maximum (*open circles*) and PL intensity (*solid circles*) on excitation photon energy for TiO_2 nanocrystals with a grain size of 12 nm

TiO_2 polycrystalline film [28]. The conversion of relevant Ti^{4+} sites to Ti^{3+} sites results in an amphiphilic surface of the TiO_2 thin film. In the present study, the surface states responsible for the observed visible emission are likely to be formed by some surface unsaturated atoms of TiO_2 nanocrystallites related to Ti^{4+}, Ti^{3+}, and Ti^{2+}, etc. These surface states can efficiently act as light absorption and emission centers. The observation of the strong radiative recombination at a low excitation power indicates that the number of the surface states is very large.

Finally, let us briefly discuss the irregularity of the change of the PL intensity with increasing grain size, i.e., with annealing treatment shown in Fig. 3. It is known that annealing treatments can cause the reduction of the number of the surface states due to the increase of grain sizes. Accordingly, the PL intensity should decrease upon annealing. However, defects inside the grains can migrate into the grain surface regions during annealing. This would increase the number of surface states, thus leading to the PL enhancement to some extent. Therefore, the PL intensity can be affected by both grain sizes and annealing treatments. Taking these two effects into account, it is possible for the PL intensity to change irregularly with annealing treatment, as shown in Fig. 3.

3 Conclusion

We have studied the PL properties of anatase TiO_2 nanocrystals fabricated by a chemical solution process. We observed strong visible emission bands with maxima from 2.15 to 2.29 eV even at excitation power as low as 0.06 W/cm^2. The PL band displayed a sublinear intensity dependence on the excitation power, a peak-position dependence on the excitation photon energy, and a large decay with irradiation time. These experimental data enable us to conclude that the observed visible luminescence in the anatase TiO_2 nanocrystals is governed by the recombination via the localized levels within the forbidden gap of some defect-related centers which presumably reside in the surface region of TiO_2 nanocrystallites. These results also show that the anatase TiO_2 nanocrystals have potential applications in photocatalysis and solar energy conversion. We are currently attempting to further understand the specificity of these surface defects and to investigate the photoelectric chemical properties of the anatase TiO_2 nanocrystals.

Acknowledgements. This work has been supported by the National Climbing Project of China.

References

1. A. Cox: Photochemistry **22**, 505 (1992)
2. R.J. Gonzalez, R. Zallen: Amorphous Insulators and Semiconductors, NATO ASI Proceedings, ed. by M.F. Thorpe, M.I. Mitkova (Kluwer, Dordrecht 1997) p. 395
3. M. Graetzel: Comments Inorg. Chem. **12**, 93 (1991)
4. H. Tang, K. Prasad, R. Sanjinès, P.E. Schnid, F. Lévy: J. Appl. Phys. **75**, 2042 (1994)
5. L. Grabner, S.E. Stokowski, W.S. Brower: Phys. Rev. B **2**, 590 (1970)
6. A. Amtout, R. Leonelli: Solid State Commun. **84**, 349 (1992)
7. H. Tang, H. Berger, P.E. Schmid, F. Lévy: Solid State Commun. **87**, 847 (1993)
8. L. Forss, M. Schubnell: Appl. Phys. B **56**, 363 (1993)

9. B.O'Regan, M. Grätzel: Nature **353**, 737 (1991)
10. C.K. ormann, D.W. Bahnemann, M.B. Hoffimann: J. Phys. Chem. **92**, 5196 (1988)
11. W.T. Pawlewice, G.J. Exarhos, W.E. Conaway: Appl. Opt. **22**, 1837 (1983)
12. X.Z. Ding, X.H. Liu, Y.Z. He: J. Mater. Sci. Lett. **15**, 1789 (1996)
13. W.H. Ma, Z.H. Lu, M.S. Zhang: Appl. Phys. A **66**, 621 (1998)
14. C.A. Melendres, A. Narayanasamy, V.A. Maroni, R.W. Siegel: J. Mater. Res. **4**, 1246 (1989)
15. M.S. Zhang, Z. Yin, Q. Chen, X. Wu, X. Ji: Ferroelectrics **168**, 131 (1995)
16. D. Bersani, P.P. Lottici, X.Z. Ding: Appl. Phys. Lett. **72**, 73 (1998)
17. L.D. Zhang, C.M. Mo: Nanostruct. Mater. **6**, 831 (1995)
18. Y.C. Zhu, C.X. Ding, G.H. Ma, Z.L. Du: J. Solid State Chem. **139**, 124 (1998)
19. K. Ishikawa, K. Yoshikawa, N. Ukada: Phys. Rev. B **37**, 5852 (1988)
20. R. Rossetti, J.L. Ellison, J.M. Gibson, L.E. Brus: J. Chem. Phys. **80**, 4464 (1984)
21. T. Itoh, M. Furumiya, T. Ikehara, C. Gourdon: Solid State Commun. **73**, 271 (1990)
22. A.D. Yoffe: Adv. Phys. **42**, 173 (1993)
23. W. Shockley, W.T. Read: Phys. Rev. **87**, 835 (1952)
24. S. Fafard, R. Leon, D. Leonard, J.L. Merz, P.M. Petroff: Phys. Rev. B **52**, 5752 (1995)
25. M.J. Steer, D.J. Mowbray, W.R. Tribe, M.S. Skolnick, M.D. Sturge, M. Hopkinson, A.G. Cullis, C.R. Whitehouse, R. Murray: Phys. Rev. B **54**, 17738 (1996)
26. R. Leonelli, J.L. Brebner: Phys. Rev. B **33**, 8649 (1986)
27. A. Amtout, R. Leonelli: Solid State Commun. **84**, 349 (1992)
28. R. Wang, K. Hashimoto, A. Fujishima: Nature **388**, 431 (1997)